An adaptive design for quantized feedback control of uncertain switched linear systems

Moustakis, Niko; Yuan, Shuai; Baldi, Simone

DOI
10.1002/acs.2860

Publication date
2018

Document Version
Final published version

Published in
International Journal of Adaptive Control and Signal Processing

Citation (APA)
Moustakis, N., Yuan, S., & Baldi, S. (2018). An adaptive design for quantized feedback control of uncertain switched linear systems. *International Journal of Adaptive Control and Signal Processing*, *32*(5), 665-680. https://doi.org/10.1002/acs.2860

Important note
To cite this publication, please use the final published version (if applicable).
Please check the document version above.

Received: 25 September 2017 | Revised: 15 January 2018 | Accepted: 16 January 2018

DOI: 10.1002/acs.2860

RESEARCH ARTICLE

WILEY

An adaptive design for quantized feedback control of uncertain switched linear systems

Nikolaos Moustakis | Shuai Yuan | Simone Baldi

Delft Center for Systems and Control, Delft University of Technology, 2628 CD Delft, The Netherlands

Correspondence
Nikolaos Moustakis, Delft Center for Systems and Control, Delft University of Technology, 2628 CD Delft, The Netherlands.
Email: N.moustakis@tudelft.nl

Funding information
European Commission, Grant/Award Number: FP7-ICT-2013.3.4; Advanced Computing, Embedded and Control Systems, Grant/Award Number: 611538

Summary

This paper addresses the problem of asymptotic tracking for switched linear systems with parametric uncertainties and dwell-time switching, when input measurements are quantized due to the presence of a communication network closing the control loop. The problem is solved via a dynamic quantizer with dynamic offset that, embedded in a model reference adaptive control framework, allows the design of the adaptive adjustments for the control parameters and for the dynamic range and dynamic offset of the quantizer. The overall design is carried out via a Lyapunov-based zooming procedure, whose main feature is overcoming the need for zooming out at every switching instant, in order to compensate for the possible increment of the Lyapunov function at the switching instants. It is proven analytically that the resulting adjustments guarantee asymptotic state tracking. The proposed quantized adaptive control is applied to the piecewise linear model of the NASA Generic Transport Model aircraft linearized at multiple operating points.

KEYWORDS

asymptotic tracking, hybrid dynamic quantization, input quantization, model reference adaptive control, switched systems

1 | INTRODUCTION

Switched systems are used to model many systems, commonly referred to as hybrid systems, exhibiting an interaction between continuous and discrete dynamics. Such systems include multiagent systems,[1] automobile power trains,[2] traffic light controls,[3] power converters,[4] fault-tolerant systems,[5,6] and many more. In the recent decades, much effort has been increasingly devoted to studying stability and stabilization problems in switched systems.[7,8] Most recently, advanced robust and adaptive control methodologies have been developed for uncertain switched systems, cf the works of Allerhand and Shaked,[9,10] Zhang et al,[11] and Yuan et al[12] for robust control and other works[13-18] for adaptive control. This work is devoted to pushing forward the state-of-the-art in adaptive control of uncertain switched systems. The most evident engineering consequence of this research effort is the capability of designing reconfigurable controllers for networked control systems (NCSs), wherein the control loops are closed through a communication network. In fact, many networked-induced phenomena in NCSs like packet losses and denial of service can be described in a switched system framework.[19-22] Since control and feedback signals are exchanged among the system's components in the form of

information packages through a network, they have to be quantized. Quantization might degrade the control performance due to finite precision of the quantizer; however, in several networked engineering applications, high precision is required despite the presence of quantization. Cooperative control of vehicles,[22] power control systems,[23] and teleoperation[24] are just some examples where the quantizer and the controller must be carefully designed in order to achieve high precision.

Much attention has been devoted by the control community to stability in nonadaptive NCSs in the presence of quantization. An established approach for achieving asymptotic regulation relies on dynamic quantization mechanisms such as the one referred to as "zooming".[25,26] In this mechanism, precision is increased by "zooming in", ie, by reducing the size of the range so that the quantization resolution becomes finer while the state becomes smaller. Starting from this idea, several extensions to (nonadaptive) switched systems have been studied: Wakaiki and Yamamoto[27] designed a dynamic quantizer and a switching law with average dwell time to stabilize switched linear systems using quantized output-feedback measurements; in the work of Wang et al,[28] a switching law was proposed based on average dwell time and a dynamic quantizer to stabilize a sampled-data switched linear system considering asynchronous switching between system modes and controller modes; Zhu et al[29] considered the passivity preservation problem for switched systems with quantization effects; Wakaiki and Yamamoto[30] studied the problem of stabilizing switched linear systems with output feedback controllers based on a common Lyapunov function considering switching delays between system modes and controller modes.

From the adaptive control point of view, most results on NCSs in the presence of quantization focus on uncertain nonswitched systems: in the work of Selivanov et al,[31] a passification-based adaptive controller with quantized measurements and disturbances is considered, where ultimate boundedness can be obtained; an adaptive optimal regulator design for unknown quantized linear discrete-time systems is proposed in the work of Zhao et al[32]; in the work of Lai et al,[33] the control design is carried out by assuming the control input is wrapped in the coupling of quantization effect and a backlash nonlinearity; adaptive backstepping quantized control is carried out in the work of Zhou et al,[34] and in the work of Yu and Lin,[35] some assumptions are relaxed; sliding mode approaches with input quantization have been proposed in the works of Li and Yang[36] and Lai et al[37]; a direct adaptive controller for linear uncertain systems with a communication channel is developed in the work of Hayakawa et al[38] and extended to nonlinear uncertain systems in their other work.[39] For most adaptive approaches, only bounded tracking error is guaranteed,[40] whereas from an engineering point of view, it is clear that asymptotic tracking would be preferred because it guarantees higher precision.

Nevertheless, for switched systems, achieving asymptotic tracking in the presence of large uncertainty is a nontrivial problem, as it has been solved only recently for switched linear systems without quantization.[14] Therefore, a relevant question arises, which motivates this work: is it possible to find an adaptive design that guarantees asymptotic tracking for uncertain switched linear systems even in the presence of quantization? In this work, we present a novel zooming approach for solving this problem. The first contribution of this work comes from the class of systems we consider, namely, uncertain switched linear systems under dwell-time switching for which the asymptotic adaptive quantized problem had not been solved. The second contribution comes from a novel dynamic quantizer with dynamic offset, which does not require the quantizer to be antisymmetric with respect to the origin and allows high precision even in the tracking case. By embedding this quantizer in a model reference quantized adaptive control framework, a Lyapunov-based analysis is used to derive the adjustment laws for the control gains and for the dynamic range and dynamic offset of the quantizer. It is worth underlining that, differently from the classic quadratic Lyapunov function with a constant positive definite matrix, eg, in the works of Wakaiki and Yamamoto,[27,30] the proposed zooming mechanism does not require to zoom out at each switching instant because we use a Lyapunov function that is nonincreasing at the switching instants. This mechanism greatly simplifies zooming procedure and makes it consistent with the zooming procedure in nonswitched systems. Via a Lyapunov-based analysis, we prove that the proposed adaptive mechanism guarantees boundedness of the closed-loop signals and asymptotic convergence of the tracking error.

This paper is organized as follows. Section 2 introduces the quantized control problem. The adaptive control design is established in Section 3, and Section 4 presents the stability and tracking results. In Section 5, the proposed quantized adaptive control scheme is evaluated on the NASA Generic Transport Model (GTM) linearized at multiple operating points.

Notation. The notation used in this work is standard:

$\mathbb{R}$: the set of real numbers;
$\mathbb{R}^+$: the set of positive real numbers;
$\mathbb{N}^+$: the set of positive integers;
$\lambda_{\max}(X)$, $(\lambda_{\min}(X))$: the largest (smallest) eigenvalue of matrix X;
$\|X\| = \sqrt{\lambda_{\max}(XX^T)}$: the induced 2-norm of matrix X (the superscript T denotes the transpose of matrix X);

$\|x\| = \sqrt{\sum_{i=1}^{n} |x_i|^2}$: the Euclidean norm of a vector $x = (x_1, x_2, \dots, x_n)^T$;
$\mathrm{tr}[X]$: the trace of a square matrix X;
$\mathscr{L}_\infty$ class: a vector signal $x(\cdot) \in [0, \infty) \to \mathbb{R}^n$ is said to belong to $\mathscr{L}_\infty$ class ($x \in \mathscr{L}_\infty$), if $\max_{t\geq 0}\|x(t)\| < \infty$, $\forall t \geq 0$;
I_n: the identity matrix of size $n \times n$.

2 | PROBLEM STATEMENT

Let us consider the uncertain time-driven switched linear system

$$\dot{x}(t) = A_{\sigma(t)}x(t) + B_{\sigma(t)}g_{\eta\mu}(u(t)), \quad \sigma(t) \in \mathscr{N} = \{1, \dots, N\}, \tag{1}$$

where $x \in \mathbb{R}^n$ is the state, $u \in \mathbb{R}^q$ is the control input, $g_{\eta\mu}(u) : \mathbb{R}^q \to Q$, with $Q \subset \mathbb{R}^q$, is the input quantizer (to be defined later), and $\sigma(\cdot)$ is a piecewise switching law taking values in $\mathscr{N}$, where N denotes the number of subsystems. The system is uncertain because the matrices $A_p \in \mathbb{R}^{n\times n}$ and $B_p \in \mathbb{R}^{n\times q}$ are *unknown* constant matrices for all $p \in \mathscr{N}$.

The switching law $\sigma(\cdot)$ satisfies the following slowly switching constraint.

Definition 1. (Dwell-time switching[41])
A switching law defining a switching sequence $S := \{t_1, t_2, \dots\}$ is admissible with dwell time if there exists a number $\tau_d > 0$ such that $t_{i+1} - t_i \geq \tau_d$, $\forall i \in \mathbb{N}^+$. Any τ_d that satisfies these constraints is called *dwell time*, and the set of admissible with dwell-time switching laws is denoted by $\mathscr{D}(\tau_d)$.

2.1 | Switched linear reference model system and controller

Let us consider the following switched linear reference model:

$$\dot{x}_{\mathrm{m}}(t) = A_{\mathrm{m}\sigma(t)}x_{\mathrm{m}}(t) + B_{\mathrm{m}\sigma(t)}r(t), \quad \sigma(t) \in \mathscr{N}, \tag{2}$$

where $x_{\mathrm{m}} \in \mathbb{R}^n$ is the desired state vector to be asymptotically tracked and $r \in \mathbb{R}^q$ is a bounded continuous reference input signal. The matrices $A_{\mathrm{m}p} \in \mathbb{R}^{n\times n}$ and $B_{\mathrm{m}p} \in \mathbb{R}^{n\times q}$ are constant *known* matrices with $A_{\mathrm{m}p} \in \mathbb{R}^{n\times n}$ Hurwitz matrices for $p \in \mathscr{N}$.

The following assumptions are made in order to have a well-posed adaptive problem.

Assumption 1. There exist constant matrices $K^*_{\mathrm{x}p} \in \mathbb{R}^{n\times q}$ and invertible constant matrices $K^*_{\mathrm{r}p} \in \mathbb{R}^{q\times q}$ such that

$$A_{\mathrm{m}p} = A_p + B_pK^{*T}_{\mathrm{x}p}, \quad B_{\mathrm{m}p} = B_pK^*_{\mathrm{r}p}. \tag{3}$$

Assumption 2. There exist known matrices $S_p \in \mathbb{R}^{q\times q}$ such that

$$\Gamma_p = K^*_{\mathrm{r}p}S_p \tag{4}$$

are symmetric and positive definite.

Assumption 3. For each subsystem in (1), the matrices A_p and B_p belong to a known and bounded uncertainty set Θ_p.

Remark 1. Assumption 1 is required for the existence of a closed-loop that matches (1) to the reference model (2) (well-posedness). Assumption 2 generalizes the classical condition of knowing the sign of the input vector field in the multivariable case. Both assumptions are, up to now, the most relaxed conditions for ensuring closed-loop signal boundedness in multivariable adaptive control[42,43] and will be adopted also in our quantization setting. Assumption 3 is required to obtain a bound on the increasing rate of the tracking error during the zooming out phase, as it will be illustrated in Section 4.

Since A_p and B_p are unknown in (1), the control gains $K^*_{\mathrm{x}p} \in \mathbb{R}^{n\times q}$ and $K^*_{\mathrm{r}p} \in \mathbb{R}^{n\times q}$ in (3) must be estimated. Therefore, the following switched adaptive controller is applied:

$$u(t) = K^T_{\mathrm{x}\sigma(t)}(t)x(t) + K_{\mathrm{r}\sigma(t)}(t)r(t), \quad \sigma(t) \in \mathscr{N}, \tag{5}$$

where $K_{\mathrm{x}p}$ and $K_{\mathrm{r}p}$, ($p \in \mathscr{N}$), are the estimates of $K^*_{\mathrm{x}p}$ and $K^*_{\mathrm{r}p}$, respectively, that are updated by an appropriate adaptive law, which will be introduced in the next section.

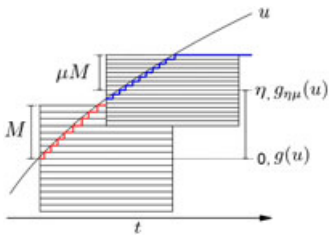

FIGURE 1 Original and quantized signals (the black line corresponds to the original signal u, the red line corresponds to quantized signal $g(u)$, and the blue line corresponds to quantized signal $g_{\eta\mu}(u)$) [Colour figure can be viewed at wileyonlinelibrary.com]

Remark 2. We consider a networked control setup with the controller on the sensor side, in which only the control input given by (5) must be quantized and sent to the actuator via a communication channel (cf Figure 2). This is a common setting in NCS literature.[20] Indeed, it is possible to consider the case in which also the system state/output is quantized. This has been addressed, eg, by Liberzon for non-uncertain systems[26]: similar methods, not explained here for lack of space, can be used also in our case of uncertain switched systems.

The next Section introduces a quantizer appropriate to our control goals.

2.2 | Dynamic quantizer design

A quantizer is a device that converts a real-valued signal into a piecewise constant one taking values in a finite set Q. The uniform static quantizer illustrated on the left side of Figure 1, with fixed quantization range M and quantization error Δ, with M, Δ positive real numbers, is represented by the function $g : \mathbb{R}^q \to Q$. The finite set of values is defined as $\{z \in \mathbb{R}^q : g(z) = i\}, i \in Q$. A common quantization choice that increases precision without sacrificing the bandwidth is adopted in the work of Liberzon,[26] where a uniform dynamic quantizer is used whose quantization range μM and quantization error $\mu\Delta$, with $\mu > 0$, can be adjusted by using a hybrid control policy.

It has to be noted that the quantizers commonly adopted in the literature are antisymmetric with respect to zero: as such, they can increase precision only around zero, and thus, they are appropriate mostly for regulation problems. If we adopted standard uniform quantizers for the tracking case, we would get

$$g(u) = g\left(K_{xp}^T x + K_{rp} r\right) = g\left(K_{xp}^T (x - x_m) + K_{xp}^T x_m + K_{rp} r\right), \tag{6}$$

where the time index t has been (and will be) omitted for compactness. From (6), we notice that, if we define the state tracking error

$$e = x - x_m, \tag{7}$$

then, for $e \to 0$, the quantized input converges to $g(K_{xp}^T x_m + K_{rp} r)$ and asymptotic tracking would be, in general, impossible due to finite precision of the quantizer around $K_{xp}^T x_m + K_{rp} r$. With this problem in mind, we introduce an adjustable offset $\eta(t) = K_{xp}^T(t) x_m(t) + K_{rp}(t) r(t)$ in the quantizer so as to achieve quantization antisymmetry with respect to η.

We define the following dynamic quantizer:

$$g_{\eta\mu}(u) = \mu g\left(\frac{u - \eta}{\mu}\right) \tag{8}$$

with $\mu > 0$. For this quantizer, we have

$$\mu g\left\|\left(\frac{u - \eta}{\mu}\right)\right\| \leq \mu M, \tag{9}$$

where μM denotes the dynamic quantization range. In case of no saturation,* the dynamic quantizer (8) must satisfy the additional requirement

$$\left\|\mu g\left(\frac{u - \eta}{\mu}\right) - u\right\| = \mu \underbrace{\left\|g\left(\frac{u - \eta}{\mu}\right) - \frac{u}{\mu}\right\|}_{\|\Delta_u\|} \leq \mu\Delta, \tag{10}$$

where $\mu\Delta$ represents the largest quantization error of the dynamic quantizer. Differences between the proposed quantizer (8) and the static uniform quantizer $g(u)$ are depicted in Figure 1. We are now ready to formulate our control objective.

*Saturation occurs when the input exceeds the maximum quantized level. In case of no saturation ($\|u - \eta\| \leq \mu M$), it holds $\|g_{\eta\mu}(u) - u\| = \mu\|\Delta_u\| \leq \mu\Delta$.

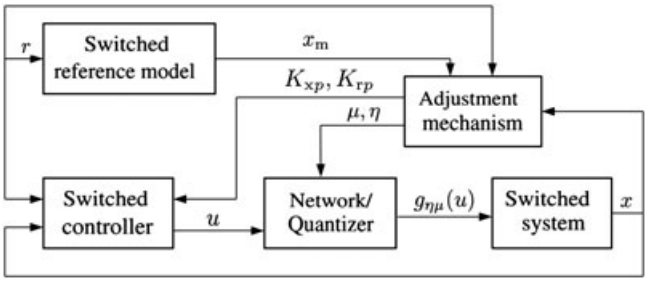

FIGURE 2 Adaptive networked control system in the model reference adaptive control framework

Problem 1. *(Input-quantized model reference adaptive control [MRAC]).* Design an adaptive control law for the control gains in (5) and adjustment strategies for the dynamic parameter μ and dynamic offset η in (8) such that, without requiring the knowledge of A_p and B_p in (1), the state trajectories of the uncertain switched system (1) track asymptotically the trajectories generated by the switched reference model (2).

A schematic representation of the proposed adaptive NCS is shown in Figure 2.

3 | ADAPTIVE LAW CONTROLLER DESIGN

In order to guarantee that the states x in (1) track x_m in (2) asymptotically, we need first to guarantee global asymptotic stability of the homogeneous part of the reference switched system (2) (ie, with $r = 0$) under a dwell-time admissible switching law $\sigma(\cdot) \in \mathscr{D}(\tau_d)$. Inspired by the works of Allerhand and Shaked[9] and Yuan et al,[14] the following lemma is stated.

Lemma 1. *The homogeneous part of the reference switched system (2) is globally asymptotically stable for any switching law $\sigma(\cdot) \in \mathscr{D}(\tau_d)$ if there exist a collection of symmetric matrices $P_{p,c} \in \mathbb{R}^{n\times n}$, $p \in \mathcal{N}$, $c = 0, 1, \dots, C$ and a sequence $\{\delta_c\}_{c=1}^{C} > 0$ with $\sum_{c=1}^{C} \delta_c = \tau_d$ such that the following inequalities hold:*

$$P_{p,c} > 0 \tag{11a}$$

$$\frac{P_{p,c+1} - P_{p,c}}{\delta_{c+1}} + P_{p,c}A_{mp} + A_{mp}^T P_{p,c} < 0 \tag{11b}$$

$$\frac{P_{p,c+1} - P_{p,c}}{\delta_{c+1}} + P_{p,c+1}A_{mp} + A_{mp}^T P_{p,c+1} < 0 \tag{11c}$$

$$c = 0, \dots, C-1$$

$$P_{p,C}A_{mp} + A_{mp}^T P_{p,C} < 0 \tag{11d}$$

$$P_{p,C} - P_{l,0} \geq 0 \tag{11e}$$

$$\forall l = 1, \dots, p-1, p+1, \dots N,$$

where C is a positive integer that determines the number of positive definite matrices to be interpolated.

By solving the linear matrix inequalities (LMIs) in (11), we obtain a collection of symmetric matrices $P_{p,c}$. This collection of matrices is used to obtain a time-varying matrix $P_p(t)$ via interpolation. The time-varying matrix $P_p(t)$, $p \in \mathcal{N}$ is defined as

$$P_p(t) = \begin{cases} P_{p,c} + \frac{P_{p,c+1} - P_{p,c}}{\delta_{c+1}}(t - t_{i,c}), & \text{for } t_{i,c} \leq t < t_{i,c+1} \\ P_{p,C} \quad , & \text{for } t_{i,C} \leq t < t_{i+1} \end{cases} \tag{12}$$

and it will be used later to define an appropriate Lyapunov function. Assume that $\sigma(t_i) = p$ and $\sigma(t_{i+1}) = l$, with $i \in \mathbb{N}^+$ and $p, l \in \mathcal{N}$. By defining a time sequence $\{t_{i,0}, \dots, t_{i,C}\}$ with $t_{i,c+1} - t_{i,c} = \delta_{c+1}$, $c = 0, \dots, C-1$ and assuming $t_{i,0} = t_i$, $t_{i,C} - t_i = \tau_d$, the time sequence between 2 switching instants t_i, t_{i+1} (and corresponding matrices $P_{p,c}$) can be seen in Figure 3. The dashed vertical lines denote the value of $P_p(t)$ at each corresponding time instant.

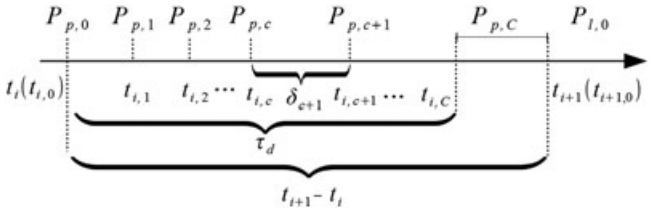

FIGURE 3 Time sequence and values of $P_p(t)$ between 2 switching instants t_i and t_{i+1}

Remark 3. The integer C in Lemma 1 can be selected a priori, depending on the allowed computational complexity. In general, $C \geq 1$ because, for $C = 0$, one has the classical quadratic Lyapunov function for which asymptotic tracking can be attained only in the presence of a common Lyapunov function.[16] For $C \geq 1$ one can create a time-varying Lyapunov function by interpolating among $C+1$ positive definite matrices. Typically, the larger the C the smaller the dwell time τ_d for which the LMIs in (11) are feasible: at the same time, the larger the C the more the decision variables in (11) (cf the work of Xiang[44] for more details).

When the quantized adaptive state-feedback controller given by (8) is applied to (1), the closed-loop system reads as

$$\begin{aligned}\dot{x}(t) = A_{\sigma(t)}x(t) + B_{\sigma(t)}\left(K_{\mathrm{x}\sigma(t)}^T x(t) + K_{\mathrm{r}\sigma(t)}r(t)\right) \\ + B_{\sigma(t)}\mu\underbrace{\left[g\left(\frac{K_{\mathrm{x}\sigma(t)}^T x(t) + K_{\mathrm{r}\sigma(t)}r(t) - \eta(t)}{\mu}\right) - \frac{K_{\mathrm{x}\sigma(t)}^T x(t) + K_{\mathrm{r}\sigma(t)}r(t)}{\mu}\right]}_{\Delta_{\mathrm{u}}},\end{aligned} \tag{13}$$

where in case of no saturation, it holds $\|\Delta_{\mathrm{u}}\| \leq \Delta$. In view of (2) and (13), the evolution of the tracking error can be written as

$$\dot{e}(t) = \dot{x}(t) - \dot{x}_{\mathrm{m}}(t) = A_{\mathrm{m}\sigma(t)}e(t) + B_{\sigma(t)}\tilde{K}_{\mathrm{x}\sigma(t)}^T x(t) + B_{\sigma(t)}\tilde{K}_{\mathrm{r}\sigma(t)}r(t) + B_{\sigma(t)}\mu\Delta_{\mathrm{u}}, \tag{14}$$

where $\tilde{K}_{\mathrm{x}p} = K_{\mathrm{x}p} - K_{\mathrm{x}p}^*$ and $\tilde{K}_{\mathrm{r}p} = K_{\mathrm{r}p} - K_{\mathrm{r}p}^*$, $p \in \mathcal{N}$, are defined as the controller parameter errors. In order to analyze the stability of the closed-loop system (14), the following Lyapunov-like function is considered:

$$V(t) = e(t)^T P_{\sigma(t)}(t)e(t) + \mathrm{tr}\sum_{p=1}^{N}\left[\tilde{K}_{\mathrm{x}p}(t)\Gamma_p^{-1}\tilde{K}_{\mathrm{x}p}^T(t)\right] + \mathrm{tr}\sum_{p=1}^{N}\left[\tilde{K}_{\mathrm{r}p}^T(t)\Gamma_p^{-1}\tilde{K}_{\mathrm{r}p}(t)\right] \tag{15}$$

with $\Gamma_p \in \mathbb{R}^{n\times n} > 0$ coming from (4). It can be seen from (12) that $P_{\sigma(\cdot)}(\cdot)$ is continuous in the time interval between 2 consecutive switches and discontinuous at switching time instants. Therefore, $V(t)$ in (15) is continuous during the interval between 2 consecutive time instants and discontinuous at switching instants.

In view of Assumption 3, lower and upper bounds for the controller parameters $K_{\mathrm{x}p}$ and $K_{\mathrm{r}p}$ can be found (this can be done by testing the matching conditions (3) over the uncertainty set Θ_p, $\forall p \in \mathcal{N}$). The parameter projection adaptive law is derived as follows:

$$\begin{aligned}\dot{K}_{\mathrm{x}\sigma(t)}^T(t) &= -S_{\sigma(t)}^T B_{\mathrm{m}\sigma(t)}^T P_{\sigma(t)}(t)e(t)x(t)^T + F_{\mathrm{x}\sigma(t)}^T \\ \dot{K}_{\mathrm{r}\sigma(t)}(t) &= -S_{\sigma(t)}^T B_{\mathrm{m}\sigma(t)}^T P_{\sigma(t)}(t)e(t)r(t)^T + F_{\mathrm{r}\sigma(t)},\end{aligned} \tag{16}$$

where $F_{\mathrm{x}p}$ and $F_{\mathrm{r}p}$ are the projection terms that keep the estimates inside the lower and upper bounds, as defined in the work of Wu et al.[45]

Remark 4. The adaptive law (16) has to be implemented as follows. Let $\{t_{p_1}^+, t_{p_2}^+, \dots\}$ represent the sequence of switch-in time instants of subsystem p, $p \in \mathcal{N}$, and let $\{t_{p_1}^-, t_{p_2}^-, \dots\}$ represent the switch-out time instants of subsystem p. The initial conditions of (16) at a switch-in time instant for subsystem p are taken from the estimates at the previous switch-out time instant of the corresponding subsystem, thus it holds $K_{\mathrm{x}p}(t_{p_{k+1}}^+) = K_{\mathrm{x}p}(t_{p_k}^-)$ and $K_{\mathrm{r}p}(t_{p_{k+1}}^+) = K_{\mathrm{r}p}(t_{p_k}^-)$, $\forall k \in \mathbb{N}^+$. Subsequently, $K_{\mathrm{x}p}$ and $K_{\mathrm{r}p}$ evolve continuously in time.

3.1 | Preliminaries in stability with slow switching

Let us consider a time interval during 2 consecutive switching instants t_i and t_{i+1}, such that $\sigma(t_i) = p$ and $\sigma(t_{i+1}) = l$, with $i \in \mathbb{N}^+$ and $p, l \in \mathcal{N}$. For $t \in [t_i, t_{i+1})$, subsystem p is active, and consequently, $K_{\mathrm{x}j}$, $K_{\mathrm{r}j}$, $\forall j \in \mathcal{N}\ /p$, are kept constant with their values identified with the values at the last switch-out instant of subsystem j, before the switching instant t_i.

Using (16) and the properties of the projection terms $F_{\mathrm{x}p}$ and $F_{\mathrm{r}p}$,[45] the time derivative of (15) along (14), during the interval $[t_i, t_{i+1})$, is

$$\dot{V} = e^T \underbrace{\left(A_{\mathrm{m}p}^T P_p + P_p A_{\mathrm{m}p} + \dot{P}_p\right)}_{-Q_p} e + \underbrace{2\mathrm{tr}\left[\tilde{K}_{\mathrm{x}p}\Gamma_p^{-1}F_{\mathrm{x}p}^T + \tilde{K}_{\mathrm{r}p}\Gamma_p^{-1}F_{\mathrm{r}p}\right]}_{K_{\mathrm{v}p}} + 2e^T P_p B_p \mu \Delta_{\mathrm{u}}, \tag{17}$$

and because $K_{\mathrm{v}p} \leq 0$,[45] (17) becomes

$$\dot{V} \leq -e^T Q_p e + 2e^T P_p B_p \mu \Delta_{\mathrm{u}}. \tag{18}$$

Because $K_{\mathrm{x}p}$ and $K_{\mathrm{r}p}$ are bounded due to the projection terms in (16), we can define $\rho \in \mathbb{R} \geq 0$ such that

$$\rho = \max_{t\geq 0} \sum_{p=1}^{N} \left\{\mathrm{tr}\left[\tilde{K}_{\mathrm{x}p}\Gamma_p^{-1}\tilde{K}_{\mathrm{x}p}^T\right] + \mathrm{tr}\left[\tilde{K}_{\mathrm{r}p}^T\Gamma_p^{-1}\tilde{K}_{\mathrm{r}p}\right]\right\}, \tag{19}$$

and because of (15), we have

$$e^T P_p e \leq V \leq e^T P_p e + \rho. \tag{20}$$

Next, we analyze the properties of $-Q_p(t)$. For $t \in [t_i, t_{i+1})$, we consider $t \in [t_{i,c}, t_{i,c+1})$, $c = 0, \ldots, C-1$. By looking at the expression of P_p in (12), one can see that $-Q_p$ can be written, in the time interval under consideration, as follows:

$$\begin{aligned} -Q_p = \lambda_1 &\left[\frac{(P_{p,c+1} - P_{p,c})}{\delta_{c+1}} + P_{p,c}A_{\mathrm{m}p} + A_{\mathrm{m}p}^T P_{p,c}\right] \\ + \lambda_2 &\left[\frac{(P_{p,c+1} - P_{p,c})}{\delta_{c+1}} + P_{p,c+1}A_{\mathrm{m}p} + A_{\mathrm{m}p}^T P_{p,c+1}\right], \end{aligned} \tag{21}$$

where $\lambda_1 = 1 - \frac{(t-t_{i,c})}{\delta_{c+1}}$, $\lambda_2 = \frac{(t-t_{i,c})}{\delta_{c+1}} > 0$. It can be seen by (11b), (11c) that

$$-Q_p(t) < 0, \text{ for } t \in [t_{i,c}, t_{i,c+1}). \tag{22}$$

Next, we consider the interval $t \in [t_{i,C}, t_{i+1})$ for the case $t_{i+1} - t_i > \tau_d$. In this case, it is true that $P_p(t) = P_{p,C}$ because of (12), and because of (11d), the following holds:

$$-Q_p(t) = A_{\mathrm{m}p}^T P_{p,C} + P_{p,C}A_{\mathrm{m}p} < 0,\ t \in [t_{i,C}, t_{i+1}). \tag{23}$$

Because of (22), (23), we have

$$-Q_p(t) < 0, \text{ for } t \in [t_i, t_{i+1}). \tag{24}$$

Let $\sigma(t_i) = p$ and $\sigma(t_{i+1}) = l$, with $i \in \mathbb{N}^+$ and $p, l \in \mathcal{N}$. At the switching instant t_{i+1}, the following holds:

$$\begin{aligned} V(t_{i+1}) - V\left(t_{i+1}^-\right) &= e^T(t_{i+1})(P_{\sigma(t_{i+1})} - P_{\sigma\left(t_{i+1}^-\right)})\, e^T(t_{i+1}) = e^T(t_{i+1})(P_{l,0} - P_{p,C})e(t_{i+1}) \\ \implies\ & V(t_{i+1}) - V\left(t_{i+1}^-\right) \leq 0. \end{aligned} \tag{25}$$

Because $K_{\mathrm{x}p}$, $K_{\mathrm{r}p}$, and e evolve continuously with respect to the time, (25) states that V in (15) is strictly decreasing in the time interval between consecutive switches and is nonincreasing at switching time instants. A situation with the proposed Lyapunov-like function (15) is shown in Figure 4.

3.2 | Preliminaries in hybrid control policy

The stable behavior of the Lyapunov function depicted in Figure 4 has now to be combined appropriately with the quantization effect. To this purpose, we have to define suitable regions where the quantizer saturates or does not saturate. Such

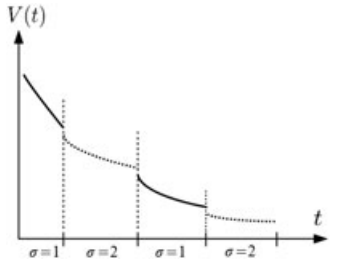

FIGURE 4 Lyapunov function $V(t)$(15), for $\sigma = \{1, 2\}$

regions will be defined based on some norm of the tracking error, as explained in the following. Because of (24), it must be true that

$$\lambda_{\min}(Q_p)\|e\|^2 \leq e^T Q_p e \leq \lambda_{\max}(Q_p)\|e\|^2,\ p \in \mathcal{N},\ t \in [t_i, t_{i+1}), \tag{26}$$

where $\lambda_{\max}(Q_p) \geq \lambda_{\min}(Q_p) > 0$. By referring to (18) and assuming no saturation in the quantizer ($\|\Delta_u\| \leq \Delta$), we are in a position to state the following:

$$\begin{aligned}
\dot{V} &\leq -\lambda_{\min}(Q_p)\|e\|^2 + 2e^T P_p B_p \mu\Delta \\
&\leq -\lambda_{\min}(Q_p)\|e\| \left(\|e\| - \underbrace{\frac{2\max\limits_{B_p\in\Theta}\|P_p B_p\|}{\lambda_{\min}(Q_p)}}_{R_p}\mu\Delta \right) \Rightarrow \\
\dot{V} &\leq -\phi\|e\|\left(\|e\| - R\mu\Delta\right)
\end{aligned} \tag{27}$$

with $\varphi = \min_{p\in\mathcal{N}}[\lambda_{\min}(Q_p)]$, $R = \max_{p\in\mathcal{N}} R_p$, where R is bounded in view of Assumption 3. According to (9), the requirement for no saturation can be equivalently expressed by

$$\|u - \eta\| \leq \mu M. \tag{28}$$

In view of the projection law (16), let us consider the well-defined bounded scalar

$$\overline{K}_{\mathrm{x}} = \max_{p\in\mathcal{N},\, t\geq 0} \|K_{\mathrm{x}p}\|. \tag{29}$$

Because $\|u - \eta\| = \|K_{\mathrm{x}p}^T x + K_{\mathrm{r}p} r - K_{\mathrm{x}p}^T x_{\mathrm{m}} - K_{\mathrm{r}p} r\| = \|K_{\mathrm{x}p}^T e\|$, the condition for no saturation is satisfied if the following condition is true:

$$\|e\| \leq \frac{\mu M}{\overline{K}_{\mathrm{x}}}. \tag{30}$$

Let us define

$$\min_{p\in\mathcal{N},\, t\in[0,\tau_p)} \left[\lambda_{\min}\left(P_p(t)\right)\right] = \xi_{\min},\ \max_{p\in\mathcal{N},\, t\in[0,\tau_p)} \left[\lambda_{\max}\left(P_p(t)\right)\right] = \xi_{\max}, \tag{31}$$

where the min and max are also taken over time, since the matrix P_p is interpolated in the interval $[0, \tau_p)$. Let us also define the following regions:

$$\begin{aligned}
\mathscr{B}_1(\mu) &:= \left\{ e(t) : \|e(t)\| \leq \frac{\mu M}{\overline{K}_{\mathrm{x}}} \right\} \\
\mathscr{I}_1(\mu) &:= \left\{ e(t) : e(t)^T P_{\sigma(t)}(t) e(t) \leq \xi_{\min} \frac{\mu^2 M^2}{\overline{K}_{\mathrm{x}}^{\,2}} \right\} \\
\mathscr{B}_2(\mu) &:= \{ e(t) : \|e(t)\| \leq \mu R\Delta \} \\
\mathscr{I}_2(\mu) &:= \left\{ e(t) : e^T(t) P_{\sigma(t)}(t) e(t) \leq \xi_{\max}\mu^2 R^2 \Delta^2 \right\}.
\end{aligned} \tag{32}$$

One can see that, if

$$\frac{\sqrt{\xi_{\min}}M}{\overline{K}_{\mathrm{x}}} > \sqrt{\xi_{\max}} R\Delta,$$

then it holds $\forall P_{\sigma(t)}(t)$, $\sigma(t) \in \mathcal{N}$, $t \geq 0$: $\mathscr{B}_2(\mu) \subset \mathscr{I}_2(\mu) \subset \mathscr{I}_1(\mu) \subset \mathscr{B}_1(\mu)$. This situation is depicted in Figure 5.

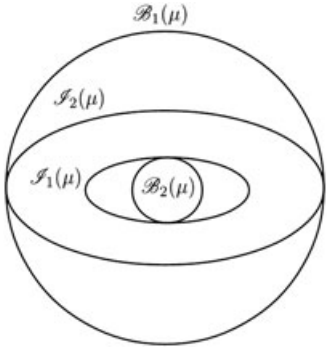

FIGURE 5 Regions of interest

4 | MAIN RESULT

Using the previously introduced concepts, the following stability and tracking result can be stated.

Theorem 1. *Consider the input-quantized MRAC given by the switched uncertain system (1), the switched reference model (2), the dynamic quantizer with adjustable offset (8), and the adaptive law (16). If the following condition holds*

$$\frac{\sqrt{\xi_{\min}}M}{\overline{K}_{\mathrm{x}}} > \sqrt{\xi_{\max}}R\Delta \tag{33}$$

(with $\xi_{\min}$, $\xi_{\max}$ defined in (31), $\overline{K}_{\mathrm{x}}$ defined in (29), and R defined after (27)), then there exists an error-based hybrid quantized feedback control policy that renders the closed-loop system (14) globally asymptotically stable with $\lim_{t\to\infty} e(t) = 0$.

Proof. The hybrid quantized feedback policy is designed in a constructive way along the proof. We distinguish 2 phases, namely, the zooming-out and zooming-in phases.[26] In the zooming-out phase, the parameter μ increases in such a way that $e \in \mathscr{B}_1(\mu)$, and thus, saturation is avoided. During the zooming-in phase, the objective is to shrink the region $\mathscr{I}_2(\mu)$ by reducing the hybrid parameter μ so that state-tracking properties can be concluded. The 2 phases are examined thoroughly as follows.

Zooming-out phase: Let $\mu(0) = 1$. If $\|e(0)\| > \frac{M}{\overline{K}_{\mathrm{x}}}$, we have saturation. In this case, we increase $\mu(t)$ fast enough to dominate the growth of e, which can be seen from (14) to be equal to $|e^{\max_{A_p,B_p\in\Theta}\|A_p+B_pK_{xp}^T\|}|$ with $\max_{A_p,B_p\in\Theta}\|A_p+B_pK_{xp}^T\|$ bounded in view of Assumption 3. There will be a time instant, call it $t_0 > 0$, at which the following relation is true:

$$\|e(t_0)\| \leq \sqrt{\frac{\xi_{\min}}{\xi_{\max}}}\frac{\mu(t_0)M}{\overline{K}_{\mathrm{x}}}, \tag{34}$$

and as a consequence of (20), (32), $e(t_0) \in I_1(\mu(t_0)) \cap \mathscr{B}_1(\mu(t_0))$. Let us take 2 consecutive switching time instants t_i and t_{i+1}, such that $\sigma(t_i) = p$, $\sigma(t_{i+1}) = l$, $p, l \in \mathscr{N}$. If $t_0 \in [t_i, t_{i+1})$, then it is true that, due to $e(t_0) \in \mathscr{B}_1(\mu(t_0))$, $\mathscr{B}_2(\mu) \subset \mathscr{B}_1(\mu)$, it holds $\dot{V} \leq 0$ from (27). As soon as $e(t_0) \in \mathscr{B}_1(\mu(t_0))$ and $\dot{V} \leq 0$, we have

$$V(t) \leq V(t_0) \implies \|e(t)\| \leq \sqrt{\frac{\mu^2(t_0)M^2}{\overline{K}_x{}^2} + \frac{\rho}{\xi_{\min}}}. \tag{35}$$

Moreover, if $t = t_{i+1}$, because e evolves continuously, (35) still holds, which implies that $e(t)$ does not necessarily decrease monotonically. Hence, for $t > t_0$, there might be 2 cases: either the norm of the tracking error is decreasing and we go to the zooming-in phase or the norm of the tracking error is increasing. For the second case, because $\mu(t)$ is increased at higher rate than the growth of $e(t)$ to avoid saturation, we can assume that $\forall t \geq t_0 \implies e(t) \in \mathscr{B}_1(\mu(t))$. As soon as V is nonincreasing at time-switching instants in view of (25), if additionally in the time interval $[t_i, t_{i+1})$ it holds $e(t) \notin \mathscr{B}_2(\mu(t))$, then it is true that $\dot{V}(t) \leq 0, \forall t \geq t_0$. In this case, because of (35), it is true that $e(t) \in \mathscr{L}_\infty, \forall t \geq t_0$.

Zooming-in phase: Let t' be a time instant such that $t \geq t' \geq t_0$ and $e(t) \in \mathscr{B}_1(\mu(t'))$. It is true, as it was shown in the zooming-out phase, that $\dot{V} \leq 0$ between time switching instants as long as $e \notin \mathscr{B}_2(\mu(t'))$, and V is nonincreasing

at switching time instants. Then, (35) holds, ie, $V(t)$ is bounded. One can see from (32) that $\mathscr{B}_2(\mu) \subset \mathscr{I}_2(\mu)$. Thus, at time $\tilde{t}$ with $\tilde{t} \geq t'$, such that $e(t') \in \mathscr{I}_2(\mu(t'))$, a zooming-in event occurs by updating $\mu(\tilde{t})$

$$\mu(\tilde{t}) = \underbrace{\frac{\overline{K}_x \sqrt{\xi_{\max}} R\Delta}{\sqrt{\xi_{\min}} M}}_{\Omega} \mu(t'). \tag{36}$$

In view of (33), it holds $\Omega < 1$. By looking at (32), one can see that $\mathscr{I}_1(\mu(\tilde{t})) = \mathscr{I}_2(\mu(t'))$. After the zooming-in event, one might have 2 cases: either the tracking error increases in which case, a new zooming-out phase is activated if e violates $e \in \mathscr{B}_1(\mu(\tilde{t}))$ or the tracking error keeps decreasing in which case, a new zooming-in event will eventually be triggered. In the second case, since μ is updated when $e \in \mathscr{I}_2(\mu)$ and because $\mathscr{B}_2(\mu) \subset \mathscr{I}_2(\mu)$, it is true that $\dot{V} \leq 0$ during the time interval between 2 consecutive switchings, as it was proven in the zooming-out phase. The following lemma will be useful to our stability analysis.

Lemma 2. (Generalized Barbalat's lemma[46])
Let $t_i \in [0, +\infty)$, $i = 1, 2, \ldots$, satisfying $t_{i+1} - t_i \leq \tau_d$. Suppose $V(t) : [0, +\infty) \to \mathbb{R}$ satisfies

1. *$\lim_{t\to\infty} V(t)$ exists;*
2. *$V(t)$ is twice differentiable in each interval $[t_i, t_{i+1})$;*
3. *$\ddot{V}(t)$ is bounded over $[0, +\infty)$ in the sense that*

$$\sup_{t_i \leq t < t_{i+1}, i=1,2,\ldots} |\ddot{V}(t)| < +\infty.$$

Then, it is true that $\lim_{t\to\infty} \dot{V}(t) = 0$.

Let us now look at the combined behavior of V during zooming-in and zooming-out phases. For $t \geq t_0$, at both zooming-in and zooming-out phases, because V is not increasing and positive, it holds $V(t)$ is upper bounded by $V(t_0)$ and lower bounded by 0. Moreover, because $\dot{V} < 0$ (for $\|e\| \neq 0$) between switching time instants if $e \notin \mathscr{B}_2(\mu)$ and because V is nonincreasing at switching time instants, it is true that $\lim_{t\to\infty} V(t)$ exists. Because V is bounded, (35) holds implying $e(t) \in \mathscr{L}_\infty$, $\forall t \geq t_0$. By looking at (17), we can conclude with similar argumentation that $\dot{e}$ is bounded because it consists of bounded terms. Additionally, because V in (15) consists of variables that evolve continuously in time, it is true that V is twice differentiable in every interval between switching time instants. Finally, by looking at the expression of $\dot{V}$ in (17), one can see that $\ddot{V}$ is bounded because it consists of bounded terms, thus it is bounded in the interval between switching time instants. As a result of the generalized Barbalat's lemma, it holds that $\lim_{t\to\infty} \dot{V}(t) = 0$.

Consequently, the following relation from (27) is true:

$$\lim_{t\to\infty} \dot{V}(t) \leq -\phi \left(\lim_{t\to\infty} \|e(t)\| \left(\|e\| - R\mu\Delta \right) \right) \implies$$
$$0 \leq -\phi \left(\lim_{t\to\infty} \|e(t)\| \left(\|e\| - R\mu\Delta \right) \right).$$

The aforementioned relation is true when

$$\lim_{t\to\infty} \|e(t)\| = 0 \text{ or } \lim_{t\to\infty} \|e(t)\| - \mu(t) R\Delta \leq 0. \tag{37}$$

The second relation in (37) implies that $e \in \mathscr{B}_2(\mu)$. However, when $e \in \mathscr{I}_2(\mu)$, a zooming-in event occurs and because $\mathscr{B}_2(\mu) \subset \mathscr{I}_2(\mu)$, it is always true that $e \notin \mathscr{B}_2(\mu)$. As a consequence $\lim_{t\to\infty} \mu(t) = 0$ and from (37), we conclude that $\lim_{t\to\infty} \|e(t)\| = 0$. Because all signals are bounded and $\lim_{t\to\infty} e(t) = 0$, we can conclude that (14) is globally asymptotically stable. □

A state flow diagram of the adaptive hybrid control strategy, with rules for zooming in/out, is shown in Figure 6.

Remark 5. Two main families of time-dependent switching that can be considered in stabilization of switched systems are slow switching and arbitrarily fast switching. While arbitrarily fast switching can handle a larger class of switching signals, it requires the existence of a common Lyapunov function that is quite conservative since a common Lyapunov function may not exist.[41] For this reason, we have considered slow switching (in particular, dwell-time switching) to handle subsystems for which a common Lyapunov function may not exist. As shown in the work of Tong et al,[16] when the reference models (2) share a common Lyapunov function, the adaptive design is greatly simplified and asymptotic stability for arbitrarily fast switching can be obtained.

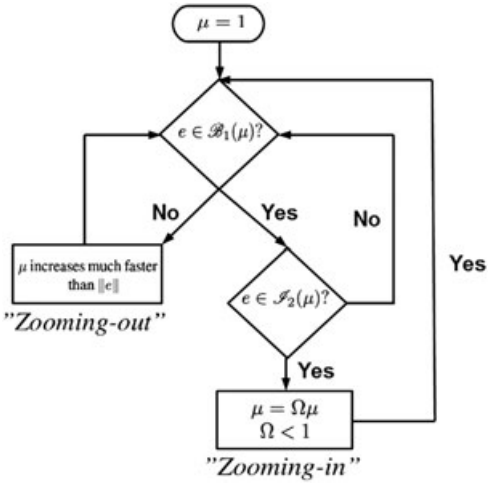

FIGURE 6 Error-dependent adaptive hybrid control strategy

Remark 6. Condition (33) relies on Assumption 3. The following guidelines are provided for checking the validity of (33): by evaluating the matching conditions (3) in the bounded uncertainty set Θ, it is possible to find the upper bound $\overline{K}_x$ to K_{xp}, $p \in \mathcal{N}$. At this point, after computing $\lambda_{\min}(Q_p)$ from (23) and with R as in (27), there always exist a static range M large enough and a number of quantization levels large enough, such that the quantization error Δ is small enough to satisfy (33). The condition (33) will lead to the constant $\Omega < 1$ in (36) to be used in the zooming-in phase. Note that different uncertainty sets Θ might lead to different quantization design parameters.

Remark 7. In the work of Wakaiki and Yamamoto,[30] a classic multiple quadratic Lyapunov function with a constant positive definite matrix was adopted. This implied that at every switching instant, it was necessary to zoom out (discontinuously), in order to compensate for the possible increment of the Lyapunov function at the switching instants. Here, the time-varying Lyapunov function (15) we adopt is nonincreasing at the switching instants, which does not require to zoom out at each switching instant to compensate possible discontinuous increments (ie, jumps). Getting rid completely of any discontinuous zooming-out phase greatly simplifies the zooming procedure and makes it consistent with the zooming procedure in nonswitched systems.[26,47]

Remark 8. It has to be underlined that, in the original nonadaptive design,[26] one can have at most a single zooming-out phase, followed by a permanent zooming-in phase due to the fact that μ decreases monotonically. However, the proof of Theorem 1 shows that, in the adaptive setting, the convergence of μ may not be monotonic. This implies multiple zooming-in and zooming-out phases, as illustrated by the following example.

5 | SIMULATION RESULTS

In this section, we study the effectiveness of the proposed adaptive hybrid control policy using the NASA GTM.[48] The nonlinear system is linearized at steady-state, straight, wings-level flight condition at 75 and 85 kt, both at 800 ft, and the resulting dynamics at each operating point are given, respectively, as follows:

$$A_1 = \begin{bmatrix} -0.0190 & 0.0825 & -0.1005 & -0.3206 \\ -0.2154 & -2.7859 & 1.2031 & -0.0271 \\ 3.2527 & -30.7871 & -3.5418 & 0 \\ 0 & 0 & 1 & 0 \end{bmatrix}, \; B_1 = \begin{bmatrix} 0.0065 & 0.0534 \\ -0.6103 & 0.0020 \\ -74.6355 & 0.5431 \\ 0 & 0 \end{bmatrix}$$

$$A_2 = \begin{bmatrix} -0.0312 & 0.1095 & -0.0938 & -0.3210 \\ -0.1057 & -3.2245 & 1.3765 & -0.0217 \\ 3.9602 & -33.8308 & -4.0756 & 0 \\ 0 & 0 & 1 & 0 \end{bmatrix}, \; B_2 = \begin{bmatrix} 0.0032 & 0.0534 \\ -0.7821 & 0.0020 \\ -96.0149 & 0.5431 \\ 0 & 0 \end{bmatrix}.$$

In line with the design in the work of Sang and Tao,[48] the desired dynamics are selected as

$$A_{m1} = \begin{bmatrix} -0.0215 & 0.0810 & -0.0988 & -0.3180 \\ -0.0706 & -2.6377 & 1.0345 & -0.2636 \\ 20.9585 & -12.6579 & -24.1637 & -28.9269 \\ 0 & 0 & 1 & 0 \end{bmatrix}$$

$$A_{m2} = \begin{bmatrix} -0.0328 & 0.1088 & -0.0930 & -0.3196 \\ 0.0753 & -3.0601 & 1.1577 & -0.3276 \\ 26.1845 & -13.6389 & -30.9393 & -37.5452 \\ 0 & 0 & 1 & 0 \end{bmatrix}$$

with $B_{m1} = B_1$ and $B_{m2} = B_2$ for the reference model. It is important to underline that the matrices A_1, B_1, A_2, and B_2 are given for simulation purposes, while the controller design does not use the knowledge of these matrices (only the knowledge of the reference model is used). The matrices S_p, $p = 1, 2$, in (16) are chosen as $S_1 = S_2 = 0.05 \cdot I_2$, and the reference signal is chosen as $r(t) = [2\sin(0.02\pi t), 0]^T$. For a dwell time $\tau_d = 5$ seconds, we pick $C = 1$ in (11) and the matrices obtained from solving the LMIs in (11) are

$$P_{1,0} = \begin{bmatrix} 1.8426 & 0.0495 & -0.0142 & -0.5113 \\ 0.0495 & 0.2034 & -0.0064 & -0.0372 \\ -0.0142 & -0.0064 & 0.0193 & 0.0208 \\ -0.5113 & -0.0372 & 0.0208 & 0.9662 \end{bmatrix}$$

$$P_{1,1} = \begin{bmatrix} 2.5588 & 0.0174 & -0.0155 & -0.7376 \\ 0.0174 & 0.4338 & -0.0181 & -0.0097 \\ -0.0155 & -0.0181 & 0.0444 & 0.0251 \\ -0.7376 & -0.0097 & 0.0251 & 1.7162 \end{bmatrix}$$

$$P_{2,0} = \begin{bmatrix} 1.8612 & 0.0455 & -0.0108 & -0.5542 \\ 0.0455 & 0.2016 & -0.0062 & -0.0251 \\ -0.0108 & -0.0062 & 0.0182 & 0.0166 \\ -0.5542 & -0.0251 & 0.0166 & 1.0178 \end{bmatrix}$$

$$P_{2,1} = \begin{bmatrix} 2.5366 & 0.0283 & -0.0115 & -0.7328 \\ 0.0283 & 0.3913 & -0.0147 & -0.0110 \\ -0.0115 & -0.0147 & 0.0361 & 0.0197 \\ -0.7328 & -0.0110 & 0.0197 & 1.7429 \end{bmatrix}.$$

Relation (31) gives for the aforementioned Lyapunov matrices $\xi_{\min} = 0.0177$ and $\xi_{\max} = 2.9873$. In addition, we assume that the controller parameters reside between lower and upper bounds as follows: $K_{\mathrm{r}p}^{(1,2)}, K_{\mathrm{r}p}^{(2,1)} \in [-1, 1]$, $K_{\mathrm{r}p}^{(1,1)}, K_{\mathrm{r}p}^{(2,2)} \in [0.5, 1.2]$ and $K_{\mathrm{x}p}^{(i,j)} \in [-1, 1]$, $i \in [1, 4]$, $j \in [1, 2]$, $p = 1, 2$ (the notation $K^{(i,j)}$ represents the (i,j)th entry of matrix K). This leads to have $R = 26.71$. Therefore, if we take the parameters of the input quantizer $g_{\eta\mu}(u)$ in (8) to be $M = 10$ and $\Delta = 0.01$, (36) is satisfied, and Ω in (36) to be used during the zooming-in phase is computed to be $\Omega = 0.49$. Finally, by evaluating the lower and upper bounds of the controller parameters $K_{\mathrm{x}p}, K_{\mathrm{r}p}, p = \{1, 2\}$ in (3), the exponential rate of growth $\max_{A_p, B_p \in \Theta} \|A_p + B_p K_{\mathrm{x}p}^T\|$ of μ, to be used during the zooming-out phase is computed to be 56.91. For the simulations, μ initially is equal to 1, the initial tracking error is $e(0) = [2, -1, 1, 0.5]^T$, and the initial parameter estimates are chosen as

$$K_{\mathrm{x}1}(0) = \begin{bmatrix} -0.1899 & -0.1943 & 0.2210 & 0.3101 \\ -0.0142 & 0.0007 & -0.0014 & 0.0009 \end{bmatrix}^T, \; K_{\mathrm{r}1}(0) = 0.75 \cdot I_2$$

$$K_{\mathrm{x}2}(0) = \begin{bmatrix} -0.1853 & -0.1682 & 0.2238 & 0.3128 \\ -0.0138 & 0.0002 & -0.0012 & 0.0016] \end{bmatrix}^T, \; K_{\mathrm{r}2}(0) = 0.75 \cdot I_2$$

(different initial conditions might affect the transient performance, but not the asymptotic tracking result). The simulation has been conducted in MATLAB-Simulink®, and the simulation results are shown in Figures 7 to 10.

The switching sequence admissible with dwell time is shown in Figure 7, whereas Figure 8 shows the dynamic range μ. Figure 9 shows that the tracking performance of the dynamic quantizer with adjustable offset is clearly satisfactory. From Figure 8, it can be seen that the quantizer parameter μ retains its initial value for the initial 7 seconds indicating that the signal is not saturated; then, it decreases abruptly in a piecewise manner indicating that the condition $e \in \mathcal{J}_2(\mu)$ triggers (36) consecutively. Thereafter, because μ stays close to zero, we have from (10) that the quantized measurement of the input value $g_{\eta\mu}(u)$ is almost identical to the actual input value u. Thus, it holds $g_{\eta\mu}(u) \approx \eta = K_{\mathrm{x}p}^T x_{\mathrm{m}} + K_{\mathrm{r}p}$, $p \in \mathcal{N}$, which identifies with the desired input to achieve asymptotic tracking in the nonquantized switched systems MRAC case.

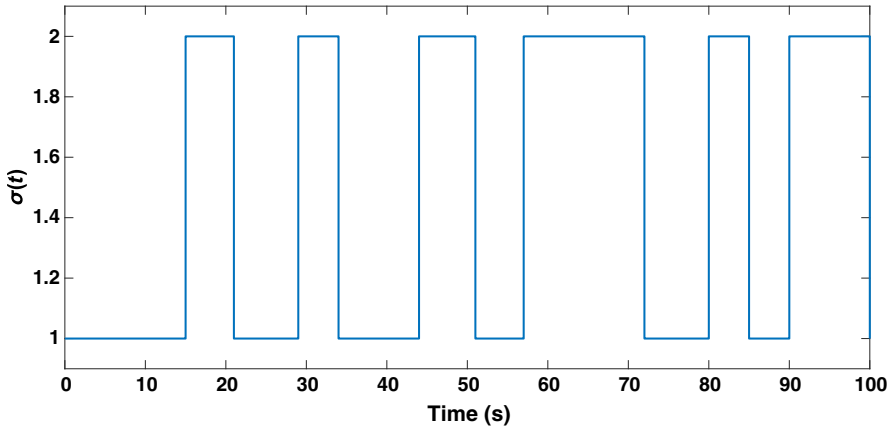

FIGURE 7 The switching signal $\sigma(t)$ [Colour figure can be viewed at wileyonlinelibrary.com]

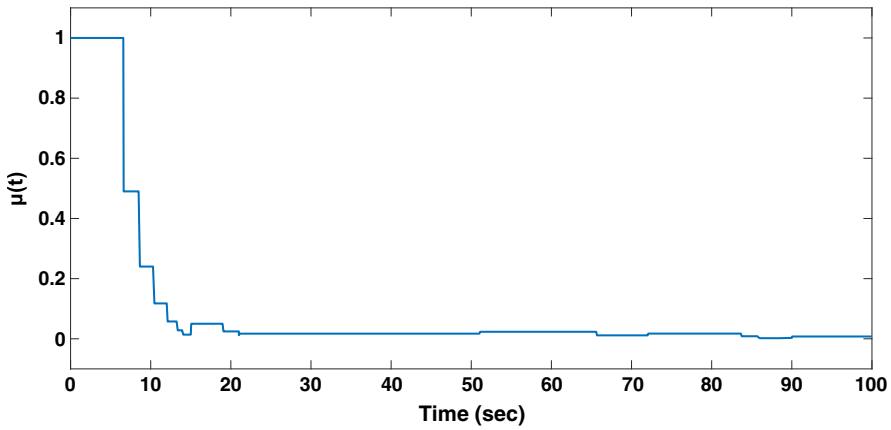

FIGURE 8 Hybrid control parameter $\mu(t)$ [Colour figure can be viewed at wileyonlinelibrary.com]

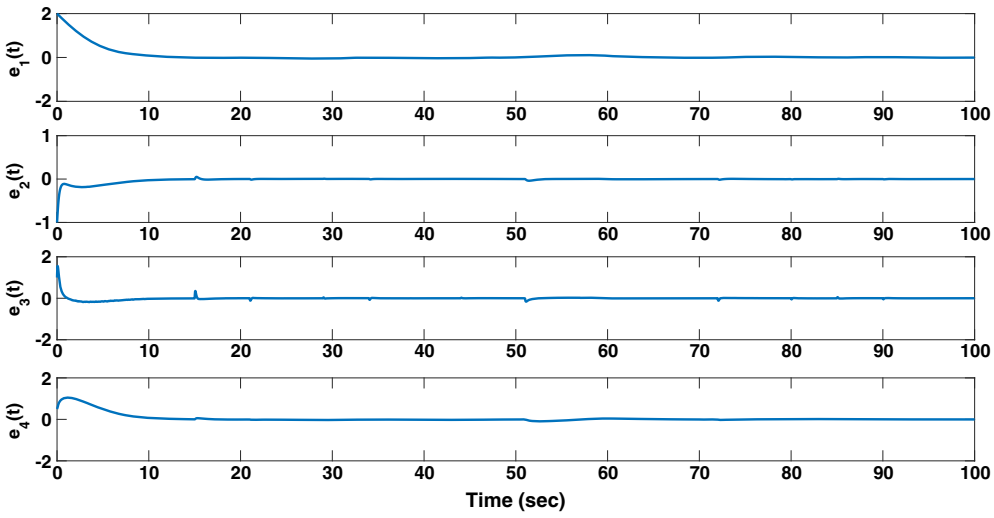

FIGURE 9 State tracking error (dynamic quantization with adaptive offset) [Colour figure can be viewed at wileyonlinelibrary.com]

It can be seen in Figure 8 that μ is not monotonically decreasing: zooming-out events occur in between zooming-in time intervals, which complies with our theoretical result in (35). In fact, zooming-out phases might occur whenever the decrease of V in (15) is caused mostly by the decrease of the parametric estimation error term: this leaves room for e to possibly increase while still having $\dot{V} \leq 0$. When e increases, $e \in \mathscr{B}_1(\mu)$ might be violated, in which case, μ increases at a faster rate than the growth of $\|e\|$ to avoid saturation.

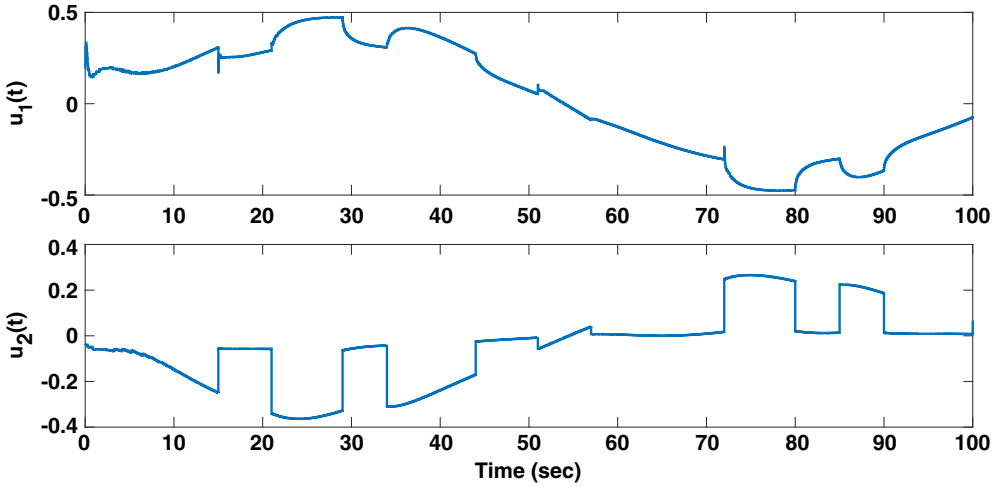

FIGURE 10 Quantized input (dynamic quantization with adaptive offset) [Colour figure can be viewed at wileyonlinelibrary.com]

6 | CONCLUSION

This work has established a novel adaptive control approach that attains asymptotic tracking for switched linear systems with parametric uncertainties and dwell-time switching, with quantized control input. In addition to enlarging the class of systems for which the adaptive quantized control can be solved, we have introduced a novel dynamic quantizer with dynamic offset to address the tracking problem. We have also used a time scheduled Lyapunov approach in an adaptive framework to avoid zooming out at every switching instant to compensate the possible increment of the Lyapunov function at the switching instants. A Lyapunov-based approach has been used to derive the adaptive adjustments for the control parameters and for the dynamic range and dynamic offset of the quantizer: the resulting (error-dependent) hybrid control policy has been given in a constructive manner, and asymptotic state tracking was shown. A practical example of the NASA GTM has been used in order to demonstrate the effectiveness of the proposed hybrid adaptive control scheme. Future work will include the extension of this approach to classes of nonlinear systems. In fact, since dynamic input quantization can be seen as a sector-bounded nonlinearity, where the sectors are defined in an adaptive way by the control gains and by the dynamic range, it is natural to explore the extension to other sector-bounded nonlinearities like saturation and dead zones.[49,50] Another relevant and challenging problem includes the study of adaptive quantized control in networked environments with asynchronous switching between the subsystems and the controllers.[8]

ACKNOWLEDGEMENTS

The research leading to these results has been partially funded by the European Commission FP7-ICT-2013.3.4, Advanced computing, embedded and control systems, under contract #611538 (LOCAL4GLOBAL).

ORCID

Nikolaos Moustakis http://orcid.org/0000-0003-2052-287X
Simone Baldi http://orcid.org/0000-0001-9752-8925

REFERENCES

1. Yang H, Jiang B, Cocquempot V, Zhang H. Stabilization of switched nonlinear systems with all unstable modes: application to multi-agent systems. *IEEE Trans Autom Control*. 2011;56(9):2230-2235.
2. Xu X, Antsaklis PJ. Optimal control of switched systems based on parameterization of the switching instants. *IEEE Trans Autom Control*. 2004;49(1):2-16.
3. Baldi S, Michailidis I, Ntampasi E, Kosmatopoulos B, Papamichail I, Papageorgiou M. A simulation-based traffic signal control for congested urban traffic networks. *Transp Sci*. Special Issue: Recent Advances in Urban Transportation Through Optimization and Analytics. 2017.
4. Loxton RC, Teo KL, Rehbock V, Ling WK. Optimal switching instants for a switched-capacitor DC/DC power converter. *Automatica*. 2009;45(4):973-980.

5. Du D, Jiang B, Shi P. Active fault-tolerant control for switched systems with time delay. *Int J Adapt Control Signal Process*. 2011;25(5):466-480.
6. Tong S, Wang T, Li Y. Fuzzy adaptive actuator failure compensation control of uncertain stochastic nonlinear systems with unmodeled dynamics. *IEEE Trans Fuzzy Syst*. 2014;22(3):563-574.
7. Shorten R, Wirth F, Mason O, Wulff K, King C. Stability criteria for switched and hybrid systems. *SIAM Rev*. 2007;49(4):545-592.
8. Zhang L, Gao H. Asynchronously switched control of switched linear systems with average dwell time. *Automatica*. 2010;46(5):953-958.
9. Allerhand LI, Shaked U. Robust state-dependent switching of linear systems with dwell time. *IEEE Trans Autom Control*. 2013;58(4):994-1001.
10. Allerhand LI, Shaked U. Robust stability and stabilization of linear switched systems with dwell time. *IEEE Trans Autom Control*. 2011;56(2):381-386.
11. Zhang L, Wang S, Karimi HR, Jasra A. Robust finite-time control of switched linear systems and application to a class of servomechanism systems. *IEEE/ASME Trans Mechatron*. 2015;20(5):2476-2485.
12. Yuan S, Zhang L, De Schutter B, Baldi S. A novel Lyapunov function for a non-weighted L_2 gain of asynchronously switched linear systems. *Automatica*. 2018;87:310-317.
13. Baldi S, Ioannou PA. Stability margins in adaptive mixing control via a Lyapunov-based switching criterion. *IEEE Trans Autom Control*. 2016;61(5):1194-1207.
14. Yuan S, De Schutter B, Baldi S. Adaptive asymptotic tracking control of uncertain time-driven switched linear systems. *IEEE Trans Autom Control*. 2017;62(11):5802-5807.
15. di Bernardo M, Montanaro U, Santini S. Hybrid model reference adaptive control of piecewise affine systems. *IEEE Trans Autom Control*. 2013;58(2):304-316.
16. Sang Q, Tao G. Adaptive control of piecewise linear systems: the state tracking case. *IEEE Trans Autom Control*. 2012;57(2):522-528.
17. Tong S, Li Y, Sui S. Adaptive fuzzy output feedback control for switched nonstrict-feedback nonlinear systems with input nonlinearities. *IEEE Trans Fuzzy Syst*. 2016;24(6):1426-1440.
18. Yuan S, De Schutter B, Baldi S. Robust adaptive tracking control of uncertain slowly switched linear systems. *Nonlinear Anal: Hybrid Syst*. 2018;27:1-12.
19. Hespanha JP, Naghshtabrizi P, Xu Y. A survey of recent results in networked control systems. *Proc IEEE*. 2007;95(1):138-162.
20. Zhang L, Gao H, Kaynak O. Network-induced constraints in networked control systems: a survey. *IEEE Trans Ind Inform*. 2013;9(1):403-416.
21. De Persis C, Tesi P. Input-to-state stabilizing control under denial-of-service. *IEEE Trans Autom Control*. 2015;60(11):2930-2944.
22. Harfouch YA, Yuan S, Baldi S. An adaptive switched control approach to heterogeneous platooning with inter-vehicle communication losses. *IEEE Trans Control Netw Syst*. 2017.
23. Su H-J, Geraniotis E. Adaptive closed-loop power control with quantized feedback and loop filtering. *IEEE Trans Wirel Commun*. 2002;1(1):76-86.
24. Kawamura K, Kobayashi Y, Fujie MG. Development of real-time simulation for workload quantization in robotic tele-surgery. Paper presented at: IEEE International Conference on Robotics and Biomimetics; 2006; Kunming, China.
25. Brockett RW, Liberzon D. Quantized feedback stabilization of linear systems. *IEEE Trans Autom Control*. 2000;45(7):1279-1289.
26. Liberzon D. Hybrid feedback stabilization of systems with quantized signals. *Automatica*. 2003;39(9):1543-1554.
27. Wakaiki M, Yamamoto Y. Quantized output feedback stabilization of switched linear systems. Paper presented at: Proceedings of the 21st International Symposium on Mathematical Theory of Networks and Systems; 2014; Groningen, The Netherlands.
28. Wang R, Xing J, Li J, Xiang Z. Finite-time quantised feedback asynchronously switched control of sampled-data switched linear systems. *Int J Syst Sci*. 2016;47(14):3320-3335.
29. Zhu F, Yu H, McCourt MJ, Antsaklis PJ. Passivity and stability of switched systems under quantization. Paper presented at: Proceedings of the 15th ACM international conference on Hybrid Systems: Computation and Control; 2012; Beijing, China.
30. Wakaiki M, Yamamoto Y. Stabilization of switched linear systems with quantized output and switching delays. *IEEE Trans Autom Control*. 2017;62(6):2958-2964.
31. Selivanov A, Fradkov A, Liberzon D. Adaptive control of passifiable linear systems with quantized measurements and bounded disturbances. *Syst Control Lett*. 2016;88:62-67.
32. Zhao Q, Xu H, Jagannathan S. Optimal control of uncertain quantized linear discrete-time systems. *Int J Adapt Control Signal Process*. 2015;29(3):325-345.
33. Lai G, Liu Z, Zhang Y, Chen CLP, Xie S. Asymmetric actuator backlash compensation in quantized adaptive control of uncertain networked nonlinear systems. *IEEE Trans Neural Netw Learn Syst*. 2017;28(2):294-307.
34. Zhou J, Wen C, Yang G. Adaptive backstepping stabilization of nonlinear uncertain systems with quantized input signal. *IEEE Trans Autom Control*. 2014;59(2):460-464.
35. Yu X, Lin Y. Adaptive backstepping quantized control for a class of nonlinear systems. *IEEE Trans Autom Control*. 2017;62(2):981-985.
36. Li Y-X, Yang G-H. Adaptive asymptotic tracking control of uncertain nonlinear systems with input quantization and actuator faults. *Automatica*. 2016;72:177-185.
37. Lai G, Liu Z, Chen CLP, Zhang Y. Adaptive asymptotic tracking control of uncertain nonlinear system with input quantization. *Syst Control Lett*. 2016;96:23-29.
38. Hayakawa T, Ishii H, Tsumura K. Adaptive quantized control for linear uncertain discrete-time systems. *Automatica*. 2009;45(3):692-700.

39. Hayakawa T, Ishii H, Tsumura K. Adaptive quantized control for nonlinear uncertain systems. *Syst Control Lett*. 2009;58(9):625-632.
40. Huang L, Li Y, Tong S. Command filter-based adaptive fuzzy backstepping control for a class of switched non-linear systems with input quantisation. *IET Control Theory Appl*. 2017;11(12):1948-1958.
41. Liberzon D. *Switching in Systems and Control*. Boston, MA: Springer Science & Business Media; 2003.
42. Tao G. *Adaptive Control Design and Analysis*. Hoboken, NJ: John Wiley & Sons; 2003.
43. Tao G. Multivariable adaptive control: a survey. *Automatica*. 2014;50(11):2737-2764.
44. Xiang W. On equivalence of two stability criteria for continuous-time switched systems with dwell time constraint. *Automatica*. 2015;54:36-40.
45. Wu C, Zhao J, Sun X-M. Adaptive tracking control for uncertain switched systems under asynchronous switching. *Int J Robust Nonlinear Control*. 2015;25(17):3457-3477.
46. Su Y, Huang J. Stability of a class of linear switching systems with applications to two consensus problems. Paper presented at: Proceedings of the 2011 American Control Conference; 2011; San Francisco, CA.
47. Yuan S, Baldi S. Stabilization of switched linear systems using quantized output feedback via dwell-time switching. Paper presented at: 2017 13th IEEE International Conference on Control and Automation (ICCA); 2017; Ohrid, Macedonia.
48. Sang Q, Tao G. Multivariable adaptive piecewise linear control design for NASA generic transport model. *J Guid Control Dyn*. 2012;35(5):1559-1567.
49. Wang T, Qiu J, Gao H. Adaptive neural control of stochastic nonlinear time-delay systems with multiple constraints. *IEEE Trans Syst Man Cybern Syst*. 2017;47(8):1875-1883.
50. Wang T, Zhang Y, Qiu J, Gao H. Adaptive fuzzy backstepping control for a class of nonlinear systems with sampled and delayed measurements. *IEEE Trans Fuzzy Syst*. 2015;23(2):302-312.

How to cite this article: Moustakis N, Yuan S, Baldi S. An adaptive design for quantized feedback control of uncertain switched linear systems. *Int J Adapt Control Signal Process*. 2018;32:665–680. https://doi.org/10.1002/acs.2860